$PM_{2.5}$ State Implementation Plan

Meteorological Modeling

Prepared by:

Utah Division of Air Quality
195 North 1950 West
Salt Lake City, Utah 84116

01 October 2013

Table of Contents

List of Figures 3
List of Tables 4
1.0 Meteorological Modeling 5
1.1 WRF Model Configuration 5
1.1.1 Modeling Domain and Resolution 5
1.1.2 Topographic Inputs and Land Use Data 12
1.1.3 Initial and Boundary Conditions 12
1.1.4 FDDA Data Assimilation 12
1.1.5 WRF Physics Options 14
1.2 WRF Performance Evaluation for 2009-2010 episode 15
1.2.1 Performance Evaluation Observational Dataset 15
1.2.2 Snow Depth and Snow Cover 16
1.2.3 Surface Temperature 19
1.2.4 Vertical Temperature Profile 23
1.2.5 Surface Wind Speed and Direction 26
1.3 Weight of Evidence (WOE)/Supplementary Analysis 34
1.3.1 Ensemble WRF/MM5 Modeling 34
1.3.2 Meteorological Modeling Sensitivities 37
1.4 Summary 38

List of Figures

Figure 1.1: The 36 km WRF Domain. Colors show topographic height in meters. 7
Figure 1.2: The 12 km WRF Domain. Colors show topographic height in meters. 8
Figure 1.3: The 4 km WRF Domain. Colors show topographic height in meters. 9
Figure 1.4: UDAQ monitoring network..... 16
Figure 1.5: Observed snow depth for 25 Dec. 2009 over the Intermountain West. 17
Figure 1.6: WRF modeled snow depth for (in meters) 25 Dec. 2009 over Northern Utah. 18
Figure 1.7: Observed snow depth for 03 Dec. 2010 over the Intermountain West. 18
Figure 1.8: WRF modeled snow depth for (in meters) 03 Jan. 2010 over Northern Utah. 19
Figure 1.9: Observed 2-meter temperature at the Logan monitor. 20
Figure 1.10: WRF modeled 2-meter temperature (red) and observed 2-meter temperature (blue) at the Hawthorne monitor. 21
Figure 1.11: WRF modeled 2-meter temperature (red) and observed 2-meter temperature (blue) at the Ogden monitor. 22
Figure 1.12: WRF modeled 2-meter temperature (red) and observed 2-meter temperature (blue) at the Lindon monitor. 22
Figure 1.13: WRF modeled 2-meter temperature (red) and observed 2-meter temperature (blue) at the Logan monitor. 23
Figure 1.14: WRF vertical temperature profile (red) and KSLC radiosonde (blue) for 18 Dec. 2009 at 00 UTC. 24
Figure 1.15: WRF vertical temperature profile (red) and KSLC radiosonde (blue) for 18 Dec. 2009 at 12 UTC. 24
Figure 1.16: WRF vertical temperature profile (red) and KSLC radiosonde (blue) for 03 Jan.. 2010 at 00 UTC. 25
Figure 1.17: WRF vertical temperature profile (red) and KSLC radiosonde (blue) for 03 Jan. 2010 at 12 UTC. 25
Figure 1.18: Averaged hourly WRF modeled 10-meter wind speed (red) and observed 10-meter wind speed (blue) at the Hawthorne monitor. 26
Figure 1.19: Averaged hourly WRF modeled 10-meter wind speed (red) and observed 10-meter wind speed (blue) at the Ogden monitor. 27
Figure 1.20: Averaged hourly WRF modeled 10-meter wind speed (red) and observed 10-meter wind speed (blue) at the Lindon monitor. 27
Figure 1.21: Averaged hourly WRF modeled 10-meter wind speed (red) and observed 10-meter wind speed (blue) at the Logan monitor. 28
Figure 1.22: Averaged hourly WRF modeled 10-meter wind direction (red) and observed 10-meter wind direction (blue) at the Hawthorne monitor. 29
Figure 1.23: Averaged hourly WRF modeled 10-meter wind direction (red) and observed 10-meter wind direction (blue) at the Ogden monitor. 30
Figure 1.24: Averaged hourly WRF modeled 10-meter wind direction (red) and observed 10-meter wind direction (blue) at the Lindon monitor. 30

Figure 1.25: Averaged hourly WRF modeled 10-meter wind direction (red) and observed 10-meter wind direction (blue) at the Logan monitor. 31
Figure 1.26: WRF wind direction (white wind barbs) and WRF topographic height (color-shaded) for 03 Jan. 2010 at midnight local time. 32
Figure 1.27: WRF wind direction (white wind barbs) and WRF topographic height (color-shaded) for 03 Jan. 2010 at 3 p.m. local time. 33
Figure 1.28: Hourly time series representing MM5 and WRF ensemble model performance for 2-m temperature for 14 – 19 Feb 2008 at the Hawthorne monitor.. 35
Figure 1.29: Hourly time series representing MM5 and WRF ensemble model performance for 2-m temperature for 14 – 19 Feb 2008 at the Logan monitor. 36
Figure 1.30: Hourly time series representing MM5 and WRF ensemble model performance for 10-m wind speed for 14 – 19 Feb 2008 at the Hawthorne monitor. 36
Figure 1.31: Hourly time series representing MM5 and WRF ensemble model performance for 10-m wind speed for 14 – 19 Feb 2008 at the Logan monitor..... 37

List of Tables

Table 1.1: Grid definitions set up in the WRF Preprocessor System (WPS). 10
Table 1.2: WRF model grid configurations, time steps, and topographic information for all three modeling domains. 10
Table 1.3: Vertical layer structure used in WRF. 11
Table 1.4: Nudging techniques used in WRF. 13
Table 1.5: Physics Options used in WRF 14
Table 1.6: WRF Performance for 2-m Temperature. 23
Table 1.7: WRF Performance for 10-meter wind speed. 28
Table 1.8: WRF Performance for 10 meter wind direction. 31
Table 1.9: The physical parameter suite used in NCAR's Ensemble Real-Time Four Dimensional Data Assimilation provided to UDAQ for February 2008 episode. 34

1.0 Meteorological Modeling

The Weather Research and Forecasting (WRF), Advanced Research WRF (WRF-ARW) model version 3.2 was used in the PM2.5 State Implementation Plan for the Salt Lake City-Ogden-Clearfield, Provo-Orem, and Logan Non-Attainment Areas. WRF contains separate modules to compute different physical processes such as surface energy budgets and soil interactions, turbulence, cloud microphysics, and atmospheric radiation. Within WRF the user has many options for selecting the different schemes for each type of physical process. There is also a WRF Preprocessing System (WPS) that generates the initial and boundary conditions used by WRF, based on topographic datasets, land use information, and larger-scale atmospheric and oceanic models.

This meteorological modeling component of the Technical Support Document will be given in three sections. First, a model configuration section will detail how WRF was configured to run the PM2.5 episode simulations. This section will include information on the modeling domain, model resolution, initial and boundary conditions, physical process schemes, and model nudging techniques. Second, a section will be dedicated to WRF model performance. Third, a section will be dedicated to additional work UDAQ performed in support of the meteorological modeling.

1.1 WRF Model Configuration

Typically, Utah's exceedances of the PM2.5 NAAQS are episodic and occur in the wintertime. The meteorological situation that leads to elevated wintertime PM2.5 begins with synoptic scale high pressure over the Intermountain Region of the U.S. Under this high pressure, stable cold air boundary layers with weak winds develop in the valley basins of the complex terrain trapping precursors (e.g., NOx) and particulates (e.g., PM2.5). These wintertime stable boundary layers are very challenging to simulate using mesoscale meteorological models. This section will detail UDAQ's configuration of WRF to simulate wintertime stable boundary layer episodes.

1.1.1 Modeling Domain and Resolution

The modeling grid, which was originally set up with the coordination of NCAR and the Army Dugway Proving Ground Division of Meteorology, uses a Lambert Conformal projection with a pole of projection of 40 degrees North, -97 degrees East and standard parallels of 33 and 45 degrees (Table 1.1).

The WRF simulations used three one-way nested horizontal with horizontal grid spacing of 36 km, 12 km, and 4 km, respectively (Table 1.2). Domain 1 covers all of the Western U.S. (Figure 1.1). Domain 2 is made up of much of the Intermountain West centered over Utah (Figure 1.2). Domain 3 encompasses the Wasatch Front of Northern Utah along with the Cache Valley that extends into Southern Idaho (Figure 1.3).

The vertical resolution is an important component in modeling wintertime cold pools. Table 1.3 gives the vertical domain in both sigma and height coordinates. This vertical resolution was chosen as it matched the NCAR's resolution for the domain they use for simulations over northern Utah. Prior to having in-house capability to run WRF, UDAQ collaborated with NCAR to provide WRF and MM5 meteorological data to support UDAQ's wintertime photochemical modeling efforts. So when UDAQ developed in-house WRF resources, it was decided to match the horizontal and vertical domain of NCAR.

There are 10 layers below 600 meters and 13 layers below 900 meters, which typically forms the top of the wintertime stable boundary layer. It is thought that increasing the vertical resolution near the surface will help the model resolve the vertical temperature structure within the boundary layer and improve wind speeds and direction. UDAQ did an exhaustive amount of sensitivity testing to analyze the effects increasing vertical resolution near the surface. There was little benefit to the WRF performance of surface temperatures, winds, and the vertical temperature profile near the surface when vertical resolution was increased in varying degrees. Also, the higher vertical resolution did not improve CMAQ photochemical modeling performance. In fact, CMAQ performance often degraded with increased vertical resolution. In the end, it was decided to use the vertical resolution presented in Table 1.3, which is the original resolution set up by NCAR.

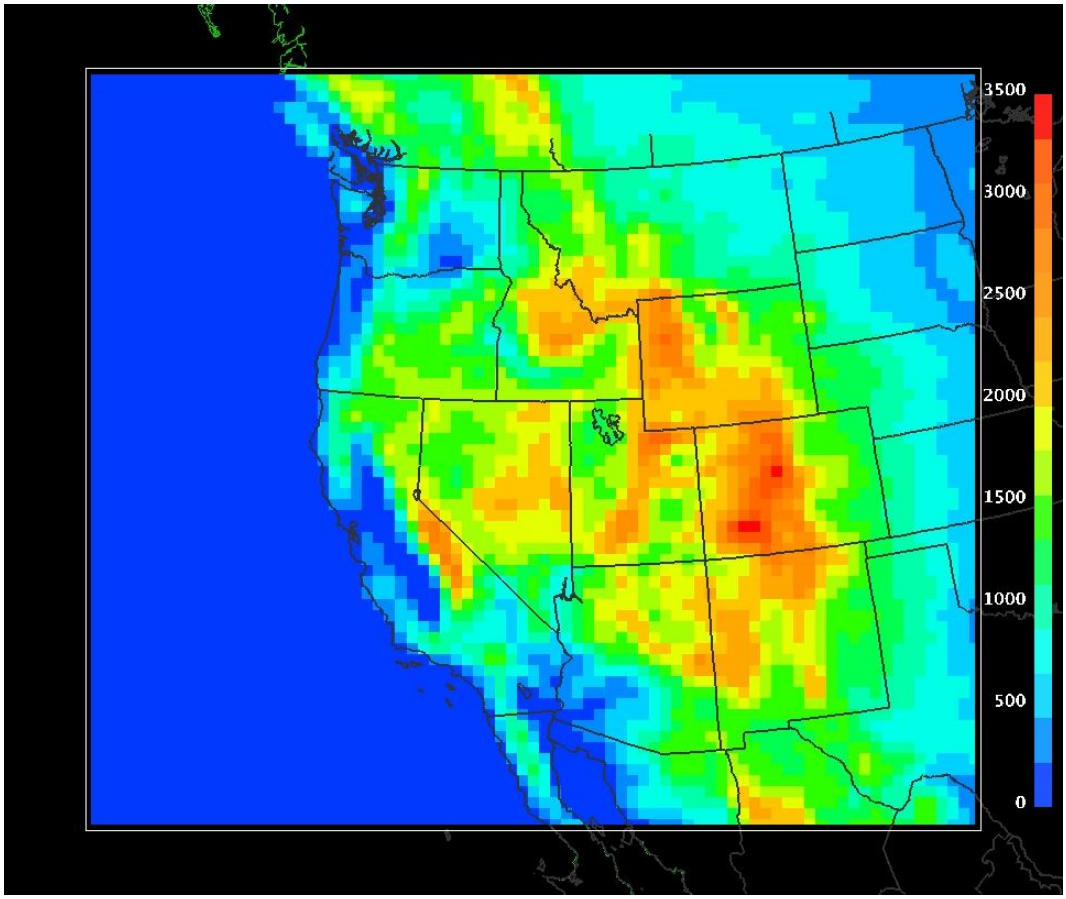

Figure 1.1: The 36 km WRF Domain. Colors show topographic height in meters.

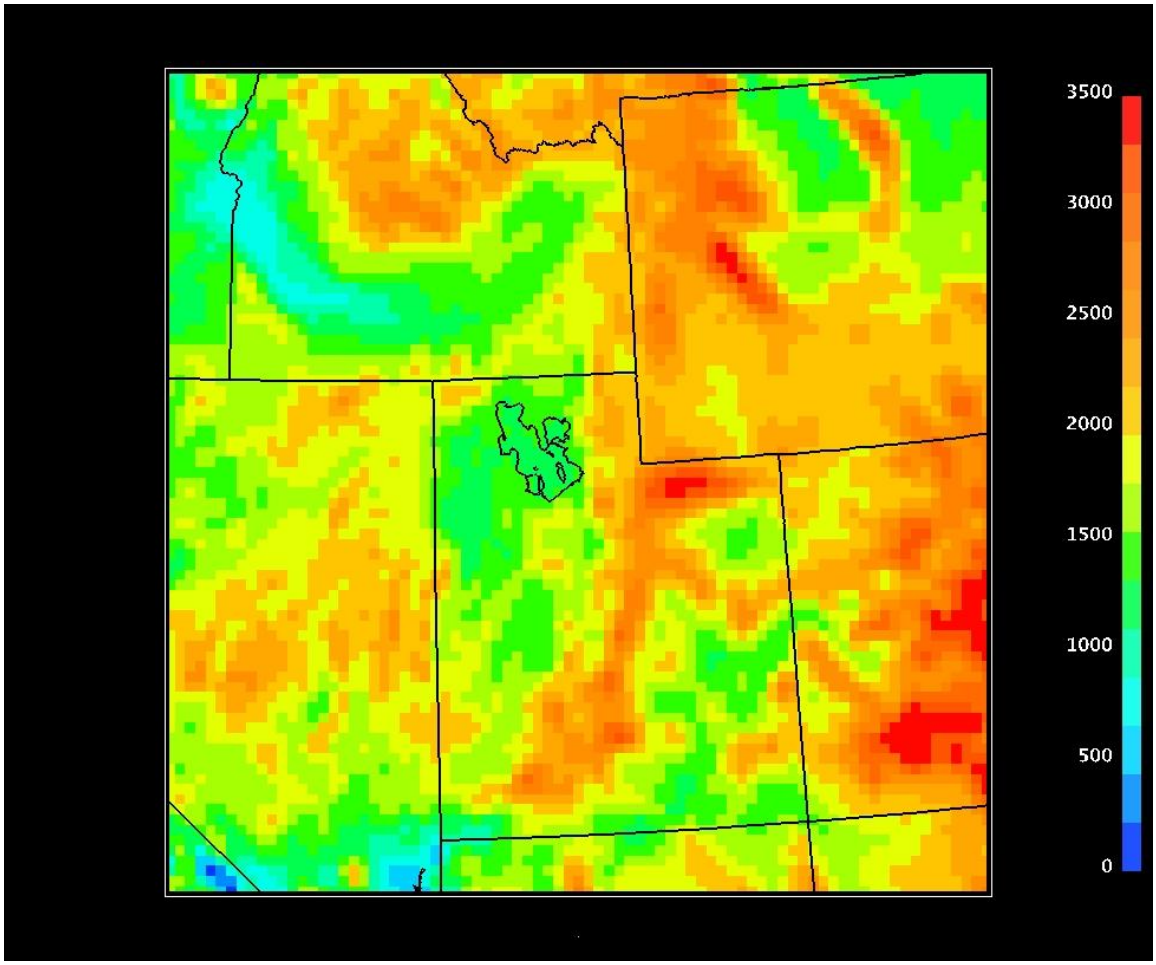

Figure 1.2: The 12 km WRF Domain. Colors show topographic height in meters.

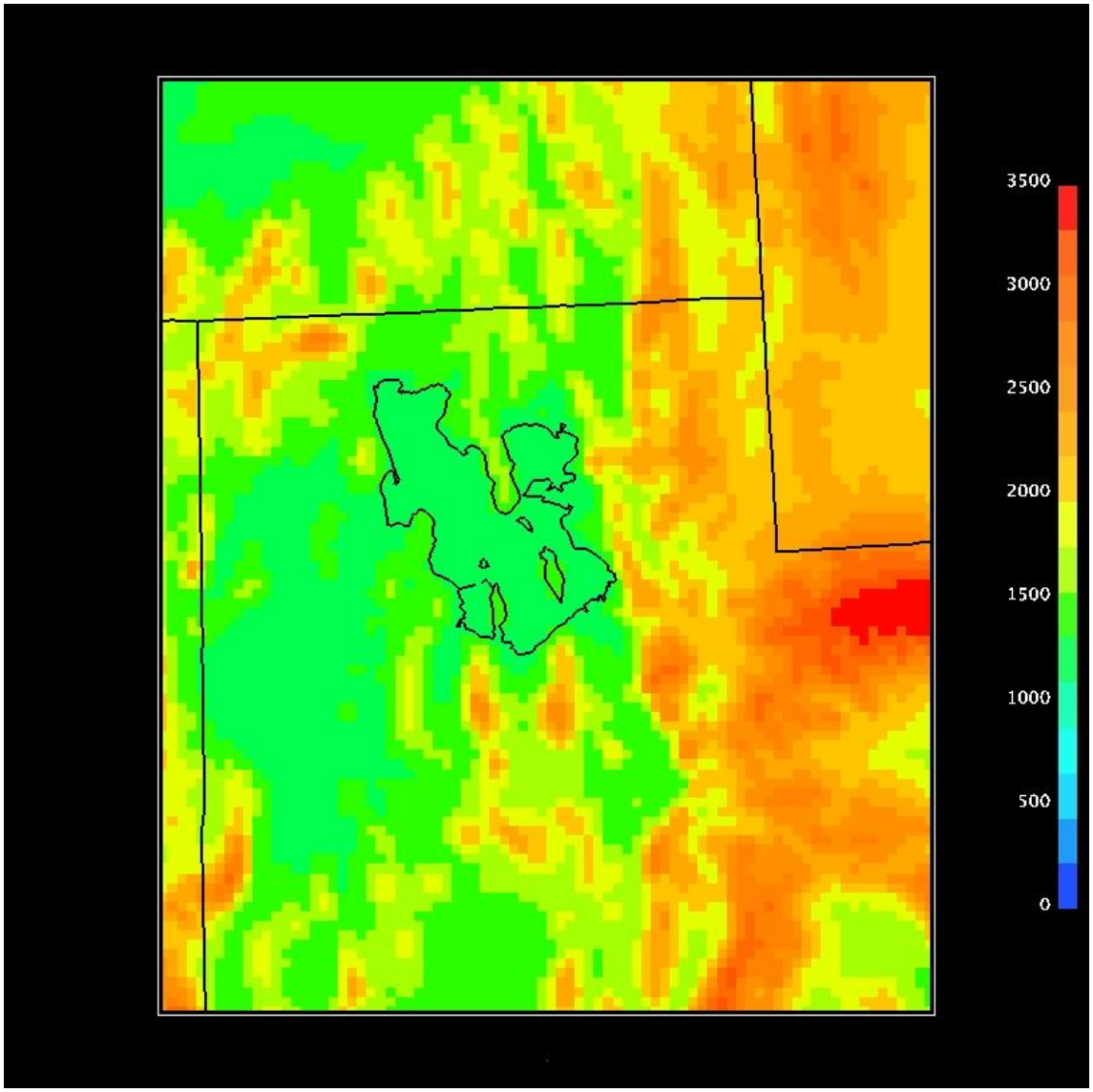

Figure 1.3: The 4 km WRF Domain. Colors show topographic height in meters.

Table 1.1: Grid definitions set up in the WRF Preprocessor System (WPS).

Projection	Lambert conformal
Reference latitude, longitude	45.0, -115.49
True latitudes	30.0, 60.0
Standard longitude	-115.490
Initial and Boundary conditions	NAM 218 Re-analysis

Table 1.2: WRF model grid configurations, time steps, and topographic information for all three modeling domains.

	Domain 1	Domain 2	Domain 3
Grid Size (x by y)	82 x 70	82 x 82	82 x 100
Horizontal Resolution (km)	36	12	4
Model Time Step (seconds)	90	30	10
Topographic Dataset	USGS 10 m	USGS 5 m	USGS 2 m
Re-Initalization Segments	5.5 days	5.5 days	5.5 days

Table 1.3: Vertical layer structure used in WRF.

Model Layer	Sigma	Height (meters)
34	0.000	14,662
33	0.050	12,822
32	0.100	11,356
31	0.150	10,127
30	0.200	9,066
29	0.250	8,127
28	0.300	7,284
27	0.350	6,517
26	0.400	5,812
25	0.450	5,160
24	0.500	4,553
23	0.550	3,948
22	0.600	3,448
21	0.650	2,942
20	0.700	2,462
19	0.740	2,095
18	0.770	1,828
17	0.800	1,569
16	0.820	1,400
15	0.840	1,235
14	0.860	1,071
13	0.880	911
12	0.900	753
11	0.910	675
10	0.920	598
9	0.930	521
8	0.940	445
7	0.950	369
6	0.960	294
5	0.970	220
4	0.980	146
3	0.985	109
2	0.990	73
1	0.995	36
	1.000	0

1.1.2 Topographic Inputs and Land Use Data

Topographic information was developed using the standard WRF databases (Table 1.2). Domain-1 was based on 10 min. global data, Domain-2 on 5 min. global data, and Domain-3 on 2 min. global data.

Vegetation type and land use information was developed using the USGS 24-category dataset that is available in the WRF Preprocessor System.

1.1.3 Initial and Boundary Conditions

The initial and Domain-1 lateral boundary conditions were obtained from the 12 km North American Model (NAM) archives from the NOAA National Operational Model Archive and Distribution System (NOMADS) website maintained by the National Climate Data Center.

1.1.4 FDDA Data Assimilation

WRF was run using Four Dimensional Data Assimilation (FDDA), applying a combination of analysis nudging, surface analysis nudging, and observational ('obs') nudging. The details of the type of nudging used on each domain and the strength of the nudging is shown in Table 1.4.

The OBSGRID module in WRF was used to produce gridded objective analyses that were used for nudging. The output files of OBSGRID can be used for 3D and surface analysis nudging and 'obs' nudging within WRF. OBSGRID takes as input raw WMO observations (both surface and upper air). It also uses the output from WPS, which consists of large-scale gridded NAM data horizontally interpolated to the model grid to be used in WRF.

For UDAQ's 4 km Domain-3, the only upper air observation available for nudging was the radiosonde launched from the Salt Lake International Airport (KSLC). The surface stations used for nudging in Domain-3 were gathered using NOAA's Meteorological Assimilation Data Ingest System (MADIS).

Analysis nudging is applied to Domain-1 and Domain-2, while 'obs' nudging is applied to the 4-km Domain-3. The 'obs' nudging of temperature and moisture are applied in the boundary layer; however the 'obs' nudging of wind is not. This is because we apply a modified surface analysis nudging technique to wind in Domain 3.

In UDAQ's WRF sensitivity analysis, 'obs' nudging of winds in the PBL was tested and showed slight improvements in WRF wind speed and direction performance. However, WRF surface winds were still bias high. UDAQ thereby used a modified surface analysis nudging technique.

The technique of using the surface analysis nudging was designed to help replicate the light near-surface wind speeds that are observed during cold pools, which WRF struggles to reproduce. The strategy was to modify the surface analysis grid file and reduce the 10 m wind speed to 25% of its original value. This was done for all gridpoints where the elevation was less than 1550 m, in order to take care of the all the valleys in the domain. For the level from 1550 m to about 2500 m, wind speed was reduced progressively less so that at 2500 m the original wind is used. The rational was to eliminate any distinct boundaries in the wind field to avoid discontinuities in the solution.

Table 1.4: Nudging techniques used in WRF.

		Domain 1	Domain 2	Domain 3
Analysis Nudging	Is it used?	Yes	Yes	No
	Strength (G) of Nudging (s-1)	0.0003	0.0003	0.0003
	Used in boundary layer	Yes	Yes	-
Surface Analysis Nudging	Is it used?	Yes	Yes	Yes*
	Strength (G) of Nudging (s-1)	0.0003	0.0003	0.0004
	Used in boundary layer	Yes	Yes	Yes
Observational Nudging	Is it used?	No	No	Yes+
	Strength (G) of Nudging (s-1)	-	-	0.0004
	Used in boundary layer	-	-	Yes

*Surface Analysis Nudging was used for just wind in Domain 3.
+Observational Nudging was used for just temperature in Domain 3.

1.1.5 WRF Physics Options

The WRF physics options that were used are given in Table 1.5. The selection of planetary boundary layer (PBL) is of importance for Utah wintertime modeling. The ACM2 (Pleim-Xiu) PBL scheme was ultimately chosen for WRF. It was chosen because it keeps consistency in the PBL schemes used in MCIP and also uses new and improved stable boundary layer code (module_bl_acm.F.SBL2010.v3). This was developed by EPA ORD and provided to UDAQ during February 2010. Other PBL schemes were tested by UDAQ, but none provided results that were improved enough to make a change from the ACM2 scheme. Since ACM2 PBL was used, the Pleim-Xiu surface layer scheme and Pleim-Xiu Land Surface Model were also chosen.

Table 1.5: Physics Options used in WRF

Physics Option	**Option Selected**
Microphysics	Lin et al. scheme
Longwave Radiation	rrtm scheme
Shortwave Radiation	Dudhia scheme
Land Surface Model (LSM)	Pleim-Xiu scheme
Planetary Boundary Layer (PBL)	ACM2 (Pleim) scheme
Surface Layer	Pleim-Xiu scheme
Cumulus parameterization	Kain-Fritsch scheme

1.2 WRF Performance Evaluation for 2009-2010 episode

This section describes the model performance evaluation (MPE) of the WRF meteorological model. The MPE will focus primarily on the meteorological properties that are important to Utah's wintertime $PM_{2.5}$ episodes. These include WRF results for snow depth, surface temperature, wind speed and direction, and the vertical temperature structure in the planetary boundary layer. The modeling period used in the model attainment demonstration is 13 Dec. 2009 – 15 Jan. 2010. It consists of four separate episodes of high $PM_{2.5}$, each containing a buildup and washout of $PM_{2.5}$.

1.2.1 Performance Evaluation Observational Dataset

UDAQ's Air Monitoring Center maintains several air monitoring sites throughout the Salt Lake City-Ogden-Clearfield, Provo-Orem, and Logan Non-Attainment Areas (Figure 3.4). These monitoring sites will provide datasets that will be used to evaluate the performance of WRF. The performance evaluation will focus on the Hawthorne and Ogden monitor for the Salt Lake City-Ogden-Clearfield NAA, the Lindon monitor for the Provo-Orem NAA, and the Logan monitor for the Logan NAA.

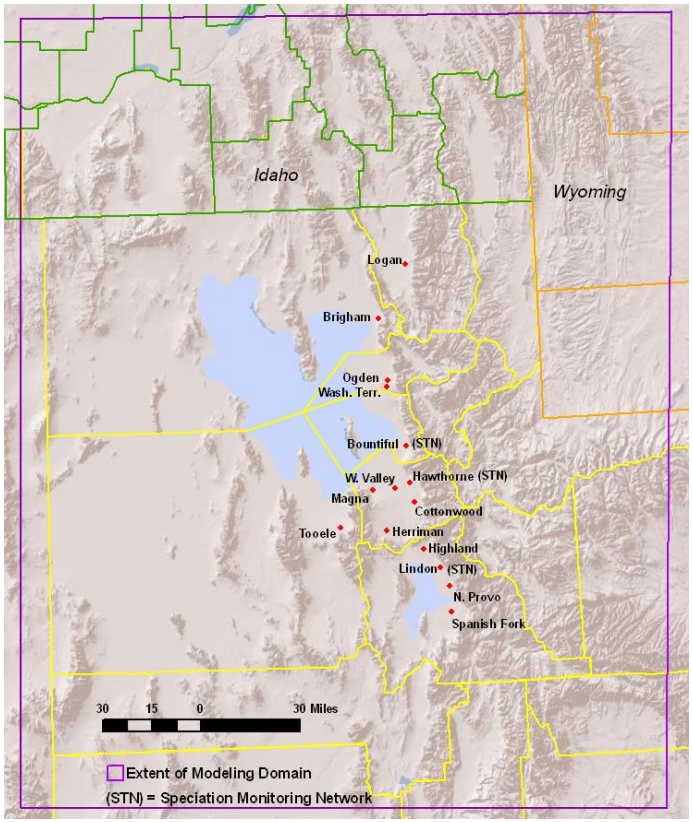

Figure 1.4: UDAQ monitoring network.

1.2.2 Snow Depth and Snow Cover

Snow depth and cover is believed to be important in the development and strength of the temperature inversions during wintertime in Utah basins. Likewise, snow depth is thought to play a significant role in the formation of secondarily formed ammonium nitrate, which makes up a large portion of the overall PM2.5 in Utah.

The observed snow depth and WRF snow depth is shown over Northern Utah in Figures 3.4 – 3.7. Figure 3.4 shows the observed snow depth for 25Dec. 2009 in inches over the Intermountain West region. It is provided by NOAA's National Operational Hydrologic Remote Sensing Center (NOHRSC). Along the Wasatch Front the observed snow depth ranges from 1 to 4 inches. There is a pocket of no snow to south of Utah Lake in Utah County and an area just south and east of the Great Salt Lake in Salt Lake and Davis Counties with a trace to 0.5 inch in snow depth. Figure 3.5 shows WRF snow depth for 25 Dec. 2009 in meters. Figure 3.5 shows WRF snow depth for 25 Dec. 2009 in meters. Snow depths in WRF range from 0.02 meters (~0.8 inches) in the western parts of the Salt Lake County basin to greater than 0.05 meters (~2 inches) in eastern Salt Lake, Utah, Davis, and Weber Counties. The lack of snow south of Utah Lake and to the immediate

south and east of the Great Salt Lake is replicated in WRF. The Cache Valley shows significant snow depth in both WRF and the observations.

Figure 3.6 shows the observed snow depth for 03 Jan. 2010 while Figure 3.7 gives WRF snow depth for the same time period. Observations and WRF snow depth are in the 1 to 4 inch range for Salt Lake, Davis, and Utah Counties for 03 Jan. 2010. The snow depth increases in both the observations and WRF to 4 to 10 inches in Weber, Box Elder, and Cache Counties.

These are two examples showing the performance of WRF snow depth. Looking throughout the 2009-2010 episode shows WRF does a reasonable job replicating snow depth over Northern Utah.

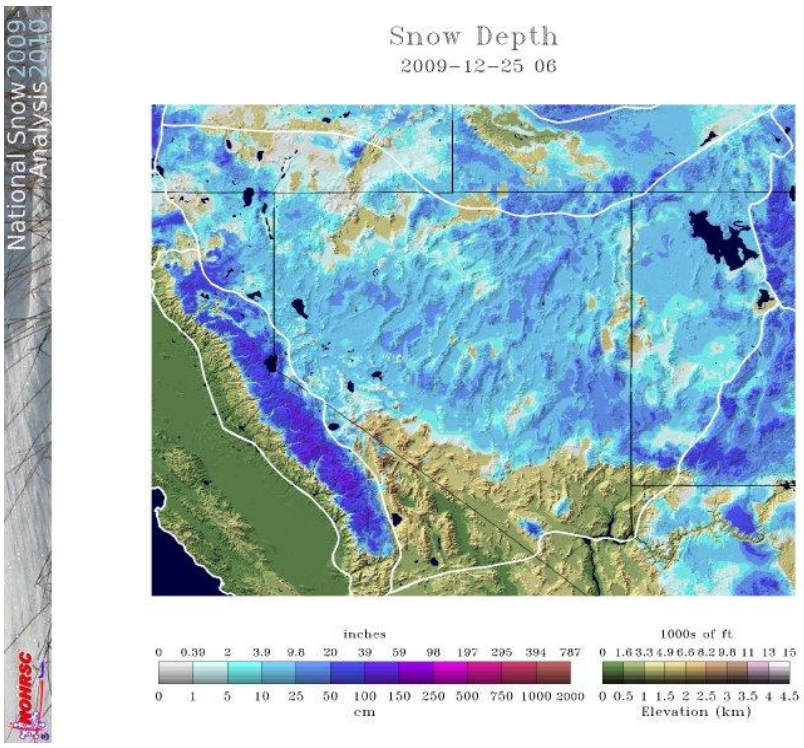

Figure 1.5: Observed snow depth for 25 Dec. 2009 over the Intermountain West.

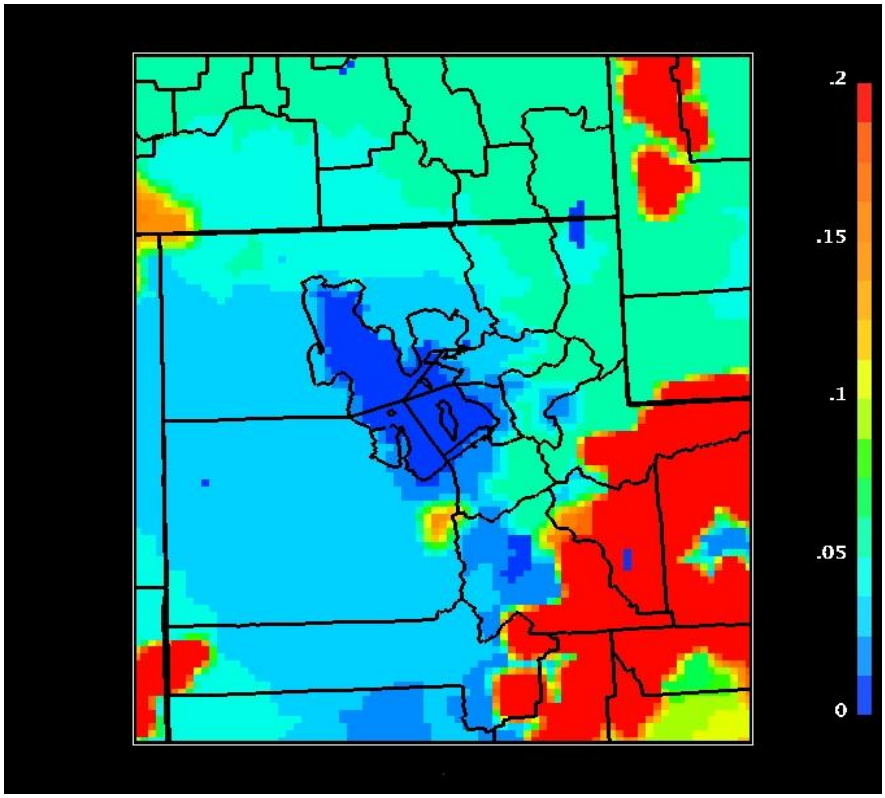

Figure 1.6: WRF modeled snow depth for (in meters) 25 Dec. 2009 over Northern Utah.

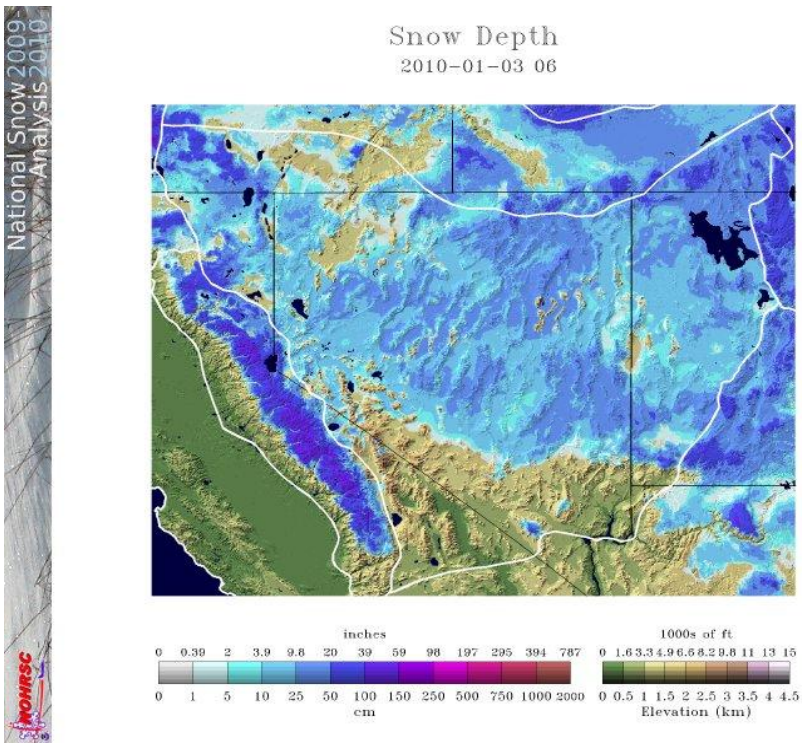

Figure 1.7: Observed snow depth for 03 Dec. 2010 over the Intermountain West.

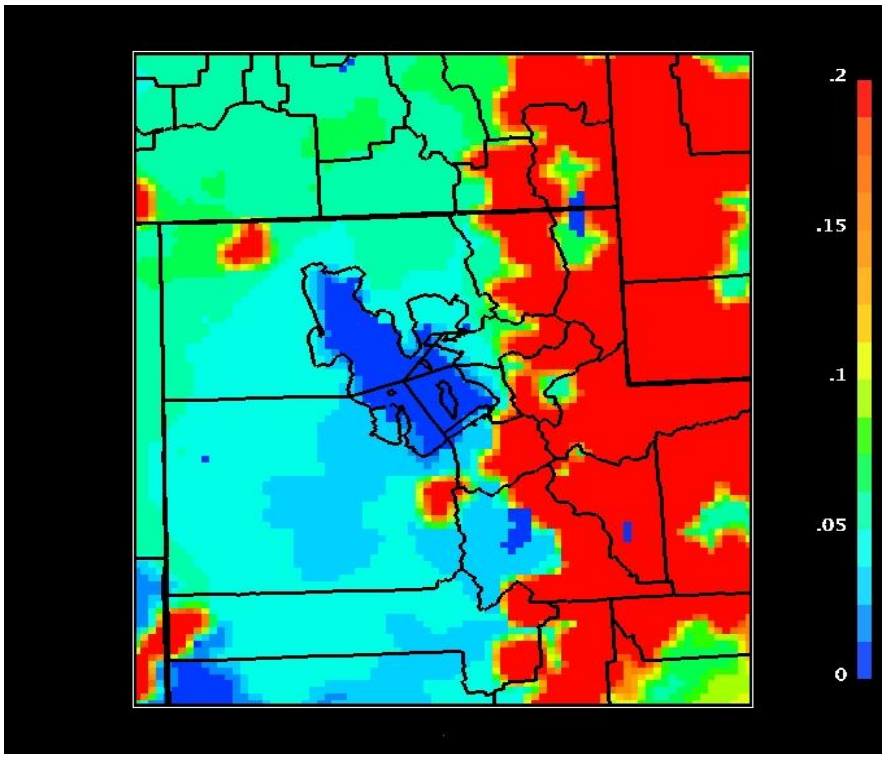

Figure 1.8: WRF modeled snow depth for (in meters) 03 Jan. 2010 over Northern Utah.

1.2.3 Surface Temperature

The surface temperature during an elevated PM2.5 episode will often exhibit a decrease in the maximum and minimum temperature from the start to the end of the episode. An example of this is shown in Figure 1.9 at Logan from 23 Dec. 2009 through 31 Dec. 2009. From the start of the episode (23 Dec. 2009) to the last day of the episode (29 Dec. 2009), the minimum and maximum daily temperatures drop each day, bottoming out at a daily maximum temperature on 29 Dec. 2009 of 11 degrees Fahrenheit. This feature in the surface temperatures is extremely challenging to replicate in WRF.

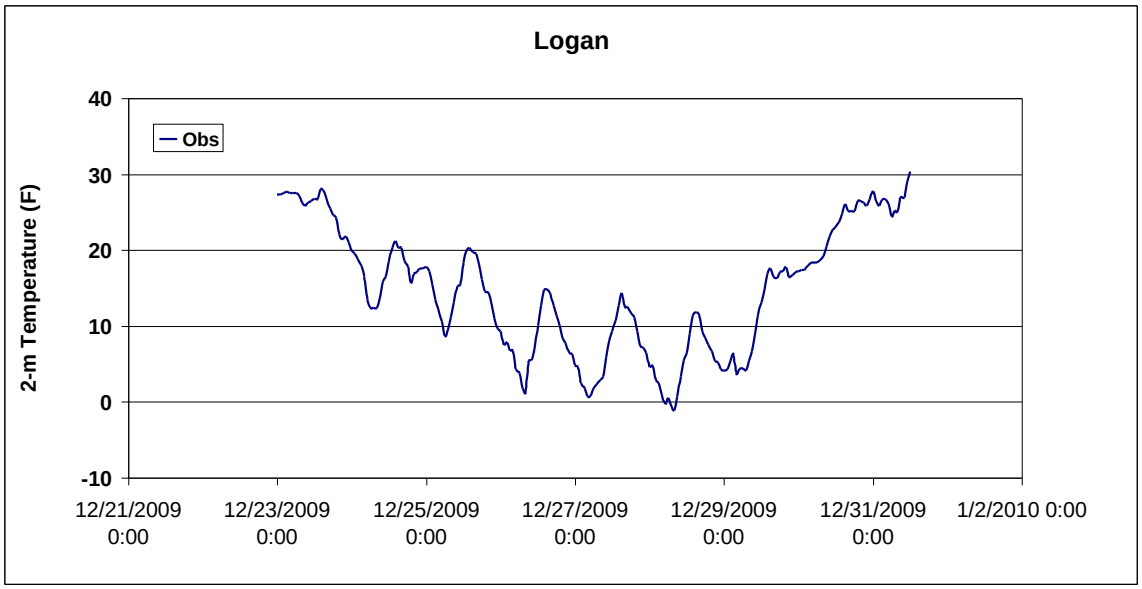

Figure 1.9: Observed 2-meter temperature at the Logan monitor.

WRF performance for 2-m temperature throughout the 2009-2010 episode is given in Figure 1.10 – 1.13.At the Hawthorne monitor, WRF (red trace) does a reasonable job of simulating the nighttime minimum temperatures (Fig. 1.10). However, WRF is much too warm during the daytime, sometimes by as much as 10 degrees at the end of PM2.5 episodes (e.g., 28 Dec. 2009). This trend of a high WRF temperature bias in daytime temperatures shows up at all locations. During these stagnant high pressure events, WRF tends to moderate the surface temperature throughout the event instead of replicating the decreasing temperatures as seen in the observations (Fig. 1.9).

There are many possible reasons for WRF's struggle in simulating surface temperatures during wintertime cold pool events. Some of the possibilities are:

- WRF PBL schemes that were not designed for complex terrain and wintertime stable boundary.
- WRF Land Surface Models that were not designed for complex terrain and wintertime stable boundary.

- The presence of an aerosol ($PM_{2.5}$) layer that will modulate the radiation in the PBL is not taken into account in WRF.

- At the end of high $PM_{2.5}$ episodes, the stable cold pool gets very shallow (~100 to 200 m above the surface) and southerly winds just above this shallow cold pool can be as fast as 10 to 20 mph. This situation would be difficult to simulate in a mesoscale model. WRF is able to replicate these strong south winds, but appears to mix the warm south to the surface leading to a destruction of the shallow stable layer and over-predicted of surface temperatures.

An evaluation of statistic metrics for 2-m temperature is presented in Table 1.6. For temperature, bias and gross error are shown for the modeling days that will be used in the Model Attainment Demonstration (see CMAQ Modeling TSD). This will eliminate days from the statistical analysis where there is poor WRF performance (i.e., the end of high $PM_{2.5}$ episodes). The results are compared to statistical benchmarks. For days that will be used in the Attainment Demonstration, WRF surface temperatures missed the traditional benchmarks established by Teshe, 2002, but are within the "complex terrain" recommended benchmark, with the exception being Logan.

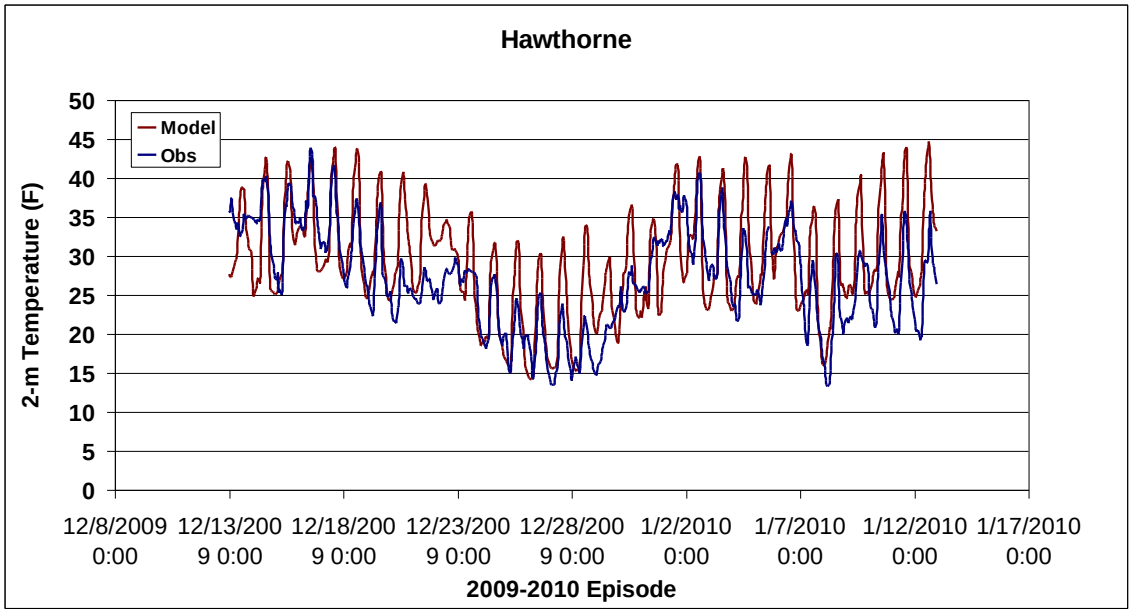

Figure 1.10: WRF modeled 2-meter temperature (red) and observed 2-meter temperature (blue) at the Hawthorne monitor.

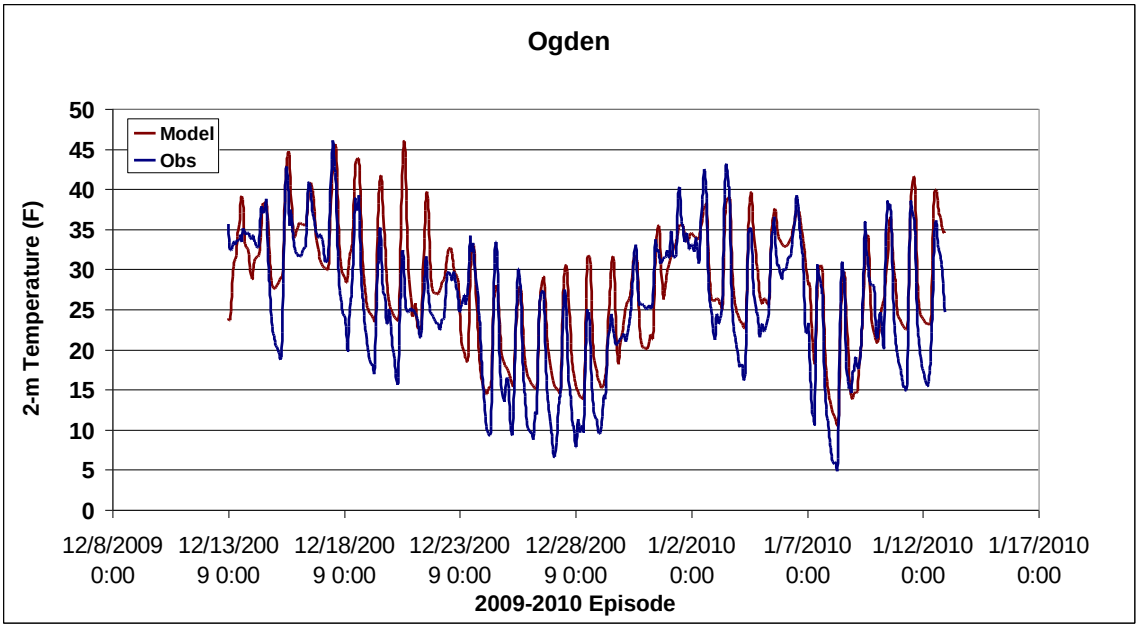

Figure 1.11: WRF modeled 2-meter temperature (red) and observed 2-meter temperature (blue) at the Ogden monitor.

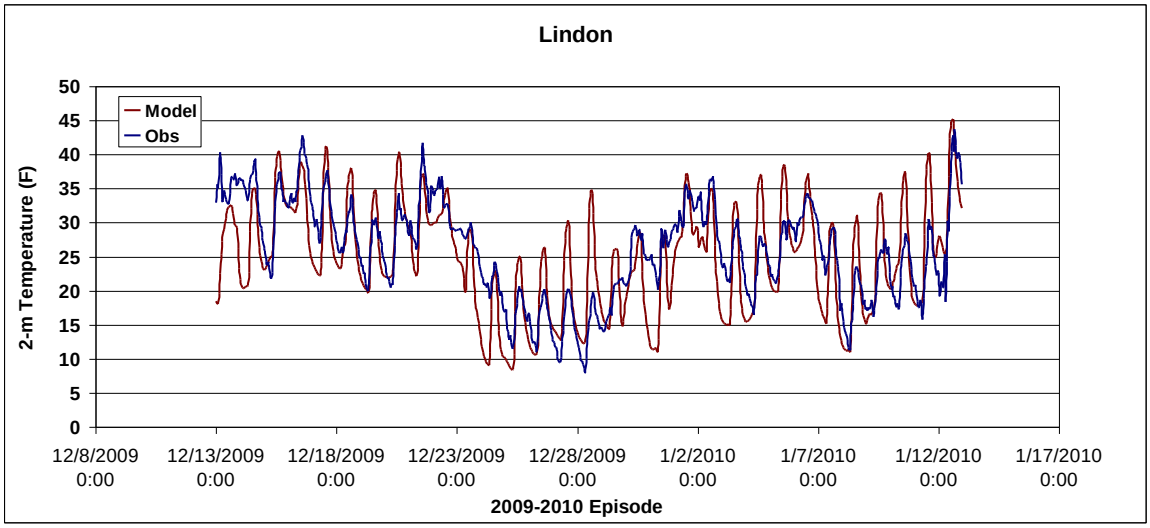

Figure 1.12: WRF modeled 2-meter temperature (red) and observed 2-meter temperature (blue) at the Lindon monitor.

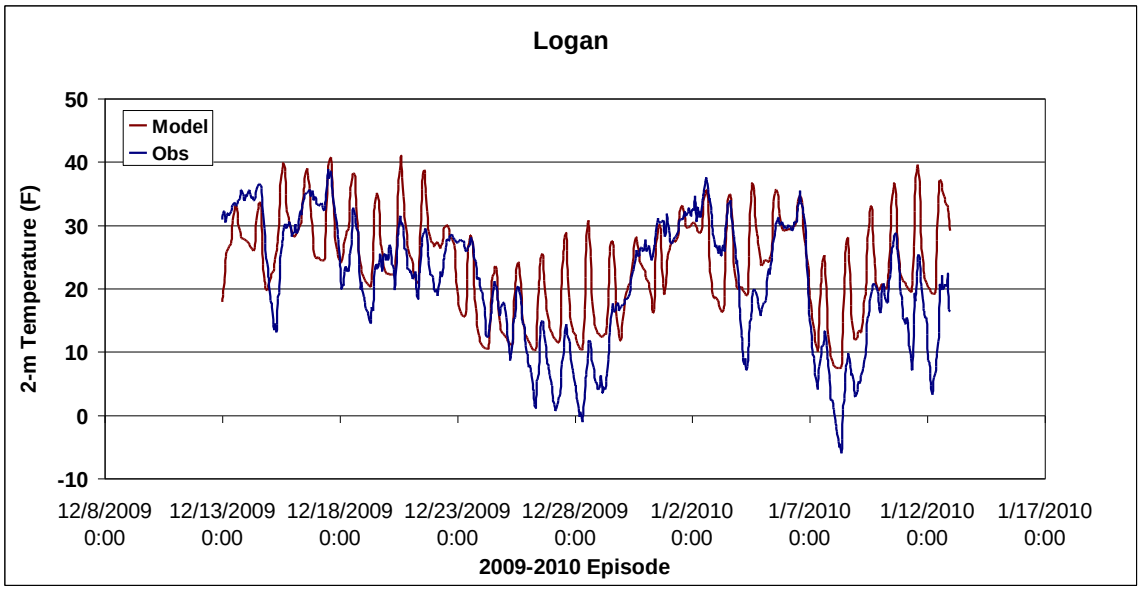

Figure 1.13: WRF modeled 2-meter temperature (red) and observed 2-meter temperature (blue) at the Logan monitor.

Table 1.6: WRF Performance for 2-m Temperature.

	Statistic – Temperature (K)	Benchmark (Teshe, 2002)	Complex Terrain Benchmark	WRF Values
Hawthorne	Bias	+- 0.5	+- 2	**1.7**
	Gross Error	<= 2	<= 3.5	**2.2**
Ogden	Bias	+- 0.5	+- 2	**1.6**
	Gross Error	<= 2	<= 3.5	**2.4**
Lindon	Bias	+- 0.5	+- 2	**0.8**
	Gross Error	<= 2	< 3.5	**2.9**
Logan	Bias	+- 0.5	+- 2	2.2
	Gross Error	<= 2	<= 3.5	**3.5**

1.2.4 Vertical Temperature Profile

The vertical temperature structure of the planetary boundary layer is important in trapping precursor emissions of PM2.5 near the surface. Measurements of the vertical profile can be obtained from a twice daily radiosonde launch at the Salt Lake City International Airport (KSLC).

Figures 1.14 – 1.17 compare the WRF vertical temperature profile to that of the radiosonde for two different days when elevated PM2.5 concentrations occurred. The WRF vertical profile in the morning (Figs. 1.15 and 1.17) show a structure and stability similar to that of the observed profile. However, WRF is typically 1 to 5 degrees warmer throughout the PBL.

Two afternoon profiles are shown by Figures 1.14 and 1.16. In the afternoon, often a mixed layer develops near the surface due to daytime heating and is capped by a valley temperature inversion between 200 and 1,000 meters above the surface. On the afternoon of 2009 Jan. 03 (Fig. 1.16), WRF performs well representing the height and stable layer between 100 and 250 meters above the surface, although the boundary is much too warm. As was the case with the morning profiles, WRF is too warm in the lower portions of the PBL.

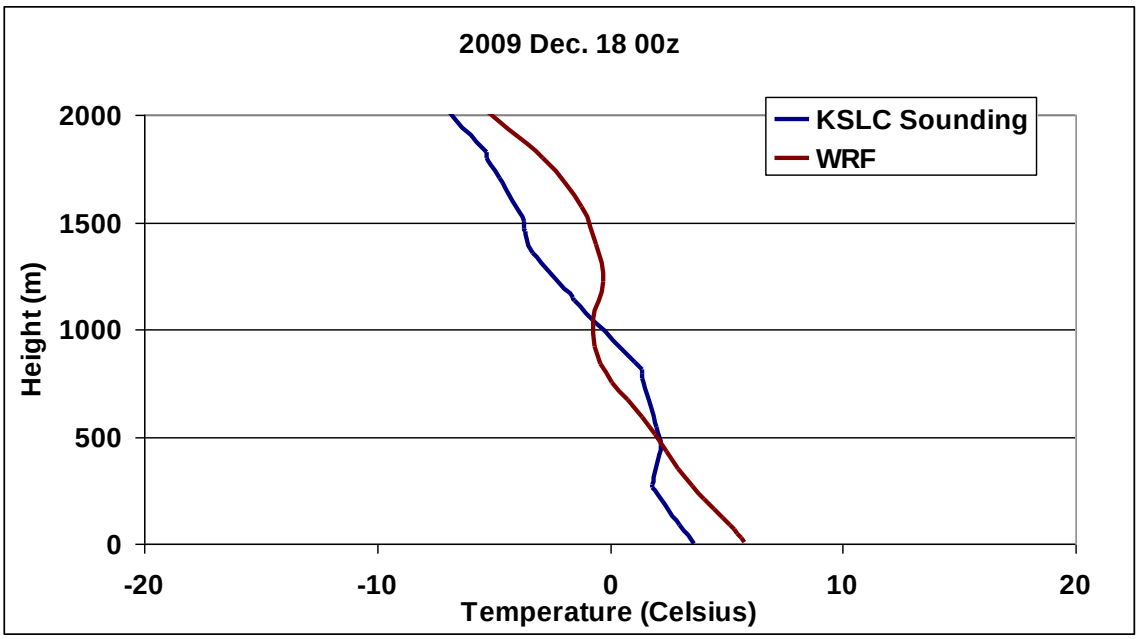

Figure 1.14: WRF vertical temperature profile (red) and KSLC radiosonde (blue) for 18 Dec. 2009 at 00 UTC.

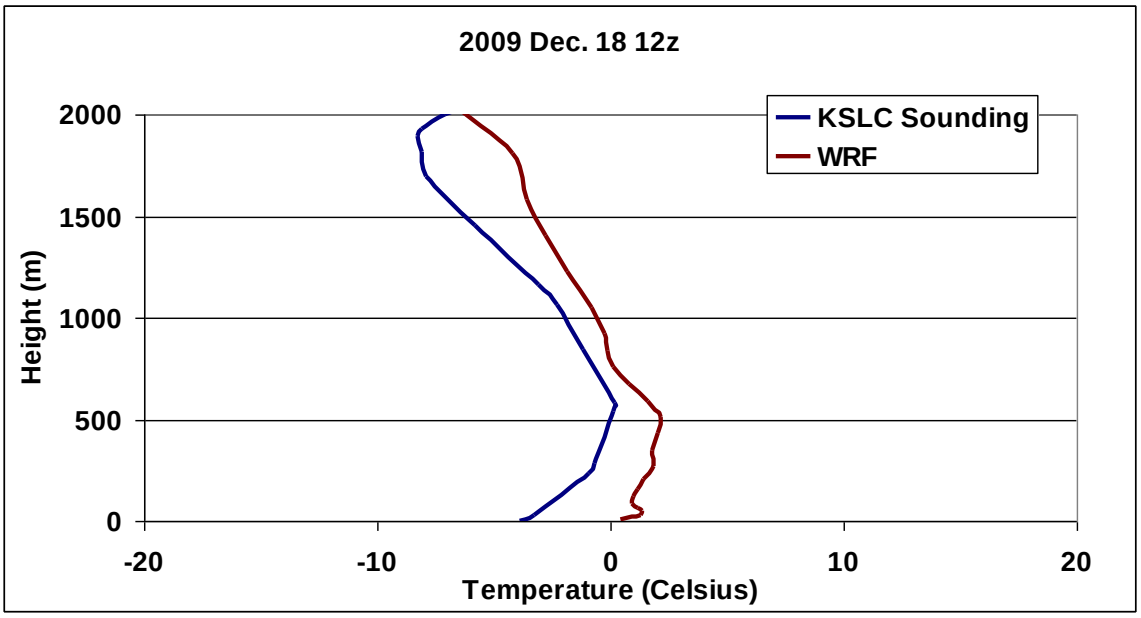

Figure 1.15: WRF vertical temperature profile (red) and KSLC radiosonde (blue) for 18 Dec. 2009 at 12 UTC.

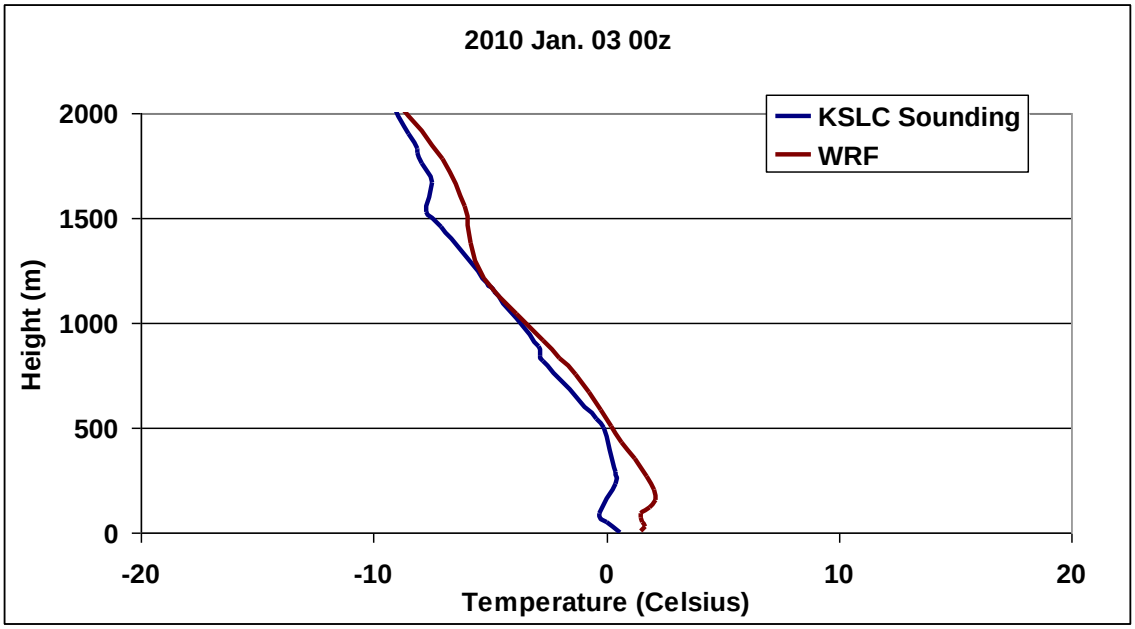

Figure 1.16: WRF vertical temperature profile (red) and KSLC radiosonde (blue) for 03 Jan.. 2010 at 00 UTC.

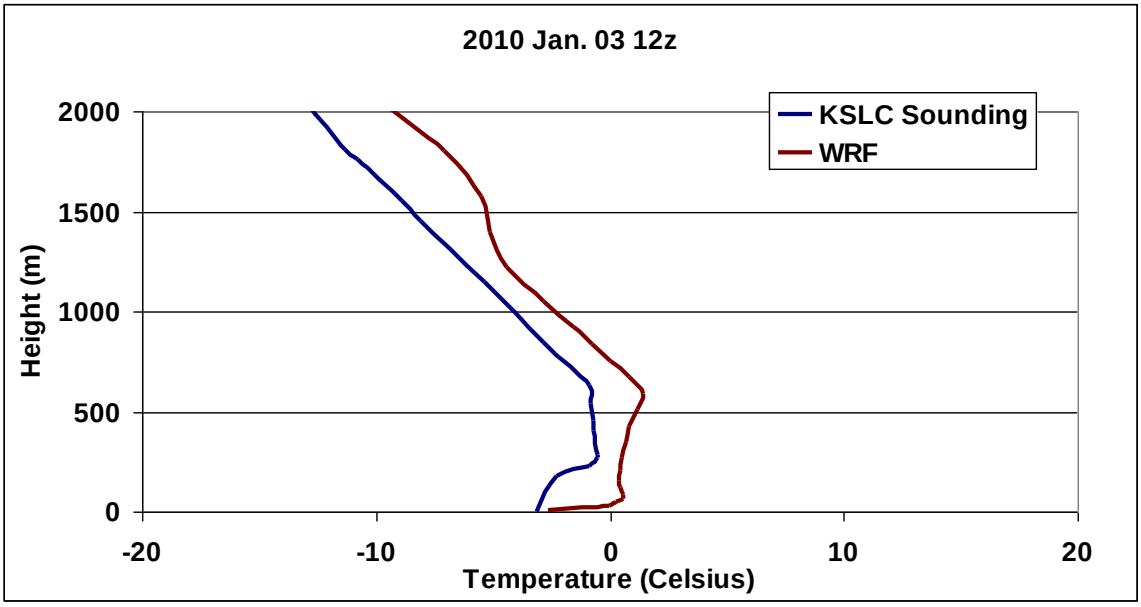

Figure 1.17: WRF vertical temperature profile (red) and KSLC radiosonde (blue) for 03 Jan. 2010 at 12 UTC.

1.2.5 Surface Wind Speed and Direction

During elevated winter PM2.5 episodes, the surface wind speeds are light (< 5 mph) and the flow is often topographically forced. During nighttime, winds typically feature a downslope flow draining to the low elevation valley bottoms. Upslope flow occurs in the afternoon, driving winds up toward the elevated terrain.

The performance of the surface wind speed and direction will be presented by averaging the hourly wind speed and direction for the days in which high concentrations of PM2.5 were observed. This was done to isolate just the elevated PM2.5 days and allows the data to be more cleanly analyzed. In all, 23 high PM2.5 days are averaged for the 2009-2010 episode.

Figures 1.18 – 1.21 give the average hourly wind speed. At all locations, the diurnal pattern in wind speed in replicated in WRF. That is, WRF reproduces the afternoon increase in winds and slower winds observed during overnight and morning hours. WRF under-estimates the nighttime wind speeds at all locations by ~ 1 mph. Before using the surface analysis FDDA technique described in Section 1.1.4, the WRF wind speed were over-estimated during all hours by ~ 1 to 3 mph. So the surface analysis FDDA technique did help improve surface wind speed performance.

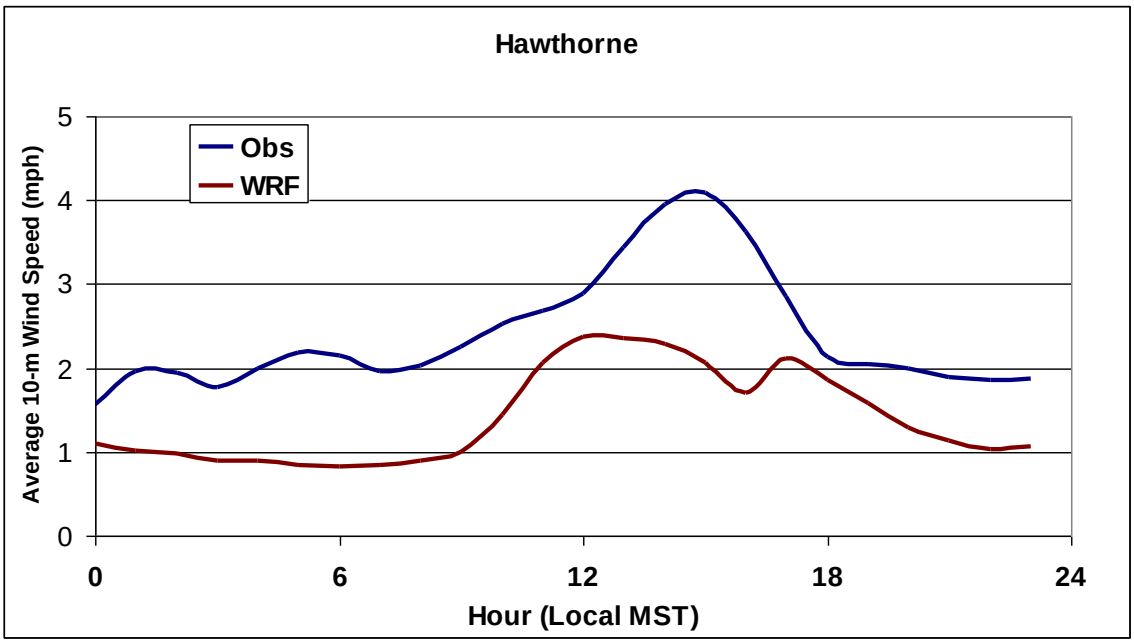

Figure 1.18: Averaged hourly WRF modeled 10-meter wind speed (red) and observed 10-meter wind speed (blue) at the Hawthorne monitor.

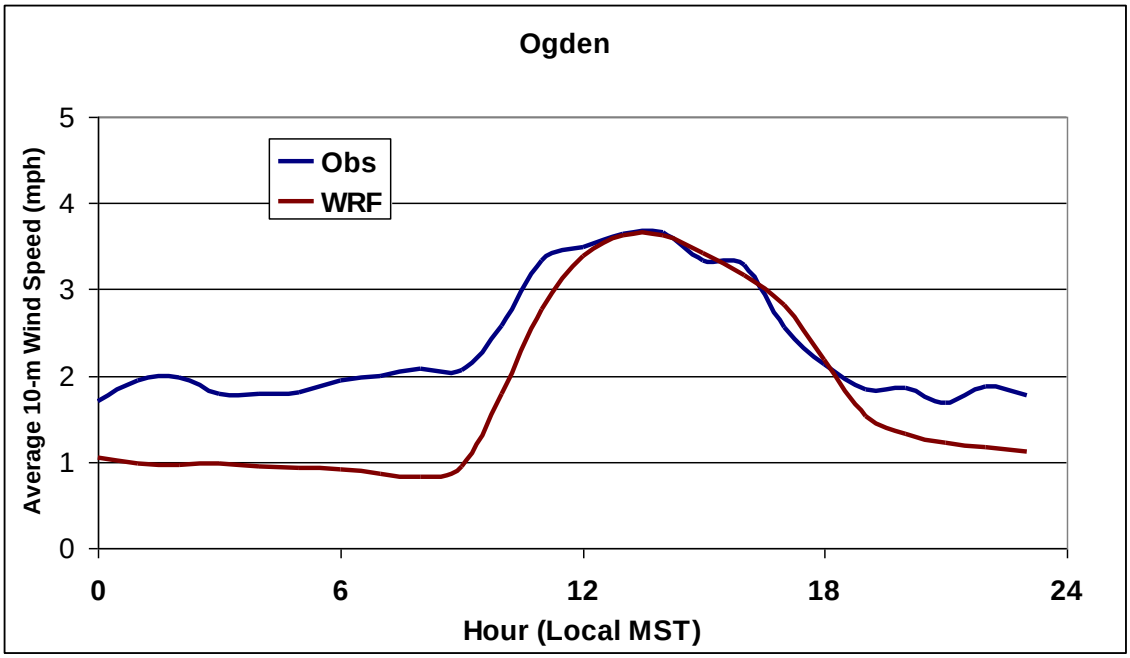

Figure 1.19: Averaged hourly WRF modeled 10-meter wind speed (red) and observed 10-meter wind speed (blue) at the Ogden monitor.

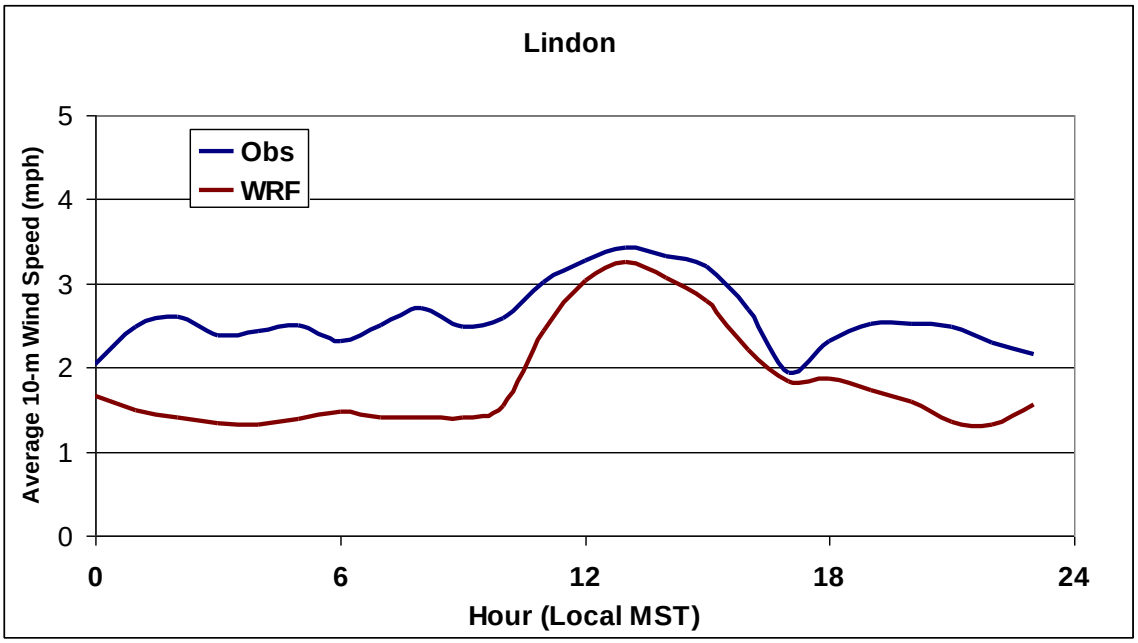

Figure 1.20: Averaged hourly WRF modeled 10-meter wind speed (red) and observed 10-meter wind speed (blue) at the Lindon monitor.

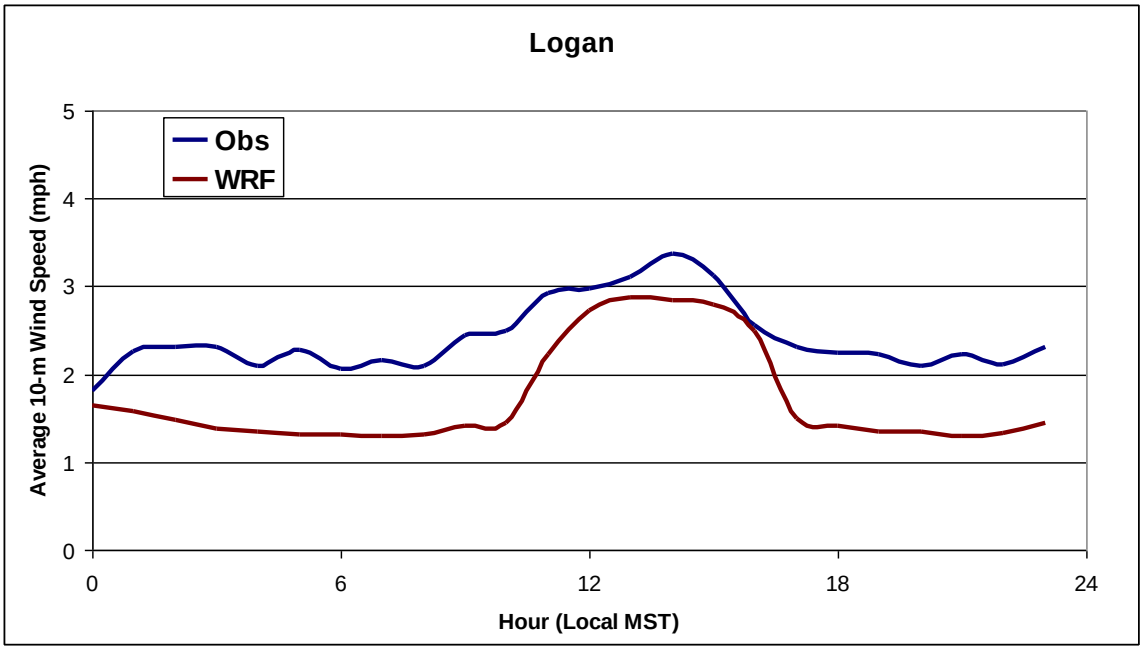

Figure 1.21: Averaged hourly WRF modeled 10-meter wind speed (red) and observed 10-meter wind speed (blue) at the Logan monitor.

An evaluation of statistic metrics for 10-m wind speed is presented in Table 1.7. For wind speed, bias and root mean square error (RMSE) are shown. Once again, the data is 'walled off' to eliminate days from the statistical analysis where there is poor WRF performance. WRF wind bias and RMSE meet traditional benchmark recommendations, with the exception being wind speed bias at Hawthorne.

Table 1.7: WRF Performance for 10-meter wind speed.

	Statistic – Wind Speed (m/s)	Benchmark (Teshe, 2002)	Complex Terrain Benchmark	WRF Values
Hawthorne	Bias	+- 0.5		-0.54
	RMSE	<= 2	<= 2.5	**0.78**
Ogden	Bias	+- 0.5		**-0.22**
	RMSE	<= 2	<= 2.5	**0.16**
Lindon	Bias	+- 0.5		**-0.29**
	RMSE	<= 2	<= 2.5	**0.32**
Logan	Bias	+- 0.5		**-0.31**
	RMSE	<= 2	<= 2.5	**0.33**

Surface wind direction performance can be seen in Figures 1.22– 1.25. WRF replicates the overnight downslope and daytime upslope wind flow quite well. At the Hawthorne monitor (Fig. 1.22), WRF reproduces the nighttime southerly flow. WRF has more of

southwest flow during the daytime as compared to the west wind direction in the observations.

At the Lindon monitor, WRF produces southerly nighttime winds while the winds are mostly southeasterly in the observations (Fig. 1.24). During the daytime, the observed southwest wind directions are simulated well by WRF.

The daytime WRF performance at the Logan monitor is good as WRF produces the near westerly upslope flow (Fig. 1.25). However, the WRF shows nighttime downslope flow from the east while the observed wind is out of the south. The representation of the topography in WRF at a 4-km horizontal resolution may explain the differences seen between the nighttime observed and WRF winds. That is, at 4-km, WRF resolution may be too coarse in some instances to accurately simulate terrain induced flow. But overall, WRF seems to picking up the diurnal upslope/downslope flows common during stagnant, high PM2.5 events.

Figure 1.26 shows the wind direction for 2010 Jan. 03 at midnight local time throughout the entire domain. The white wind barbs represent WRF wind direction and the topography is represented by the color-shaded grid. The nighttime downslope flow is evident in the Cache Valley and also along the Wasatch Front, with wind draining toward the Great Salt Lake. Likewise, Figure 1.27 shows the upslope flow during the daytime hour, this example for 2010 Jan. 03 at 3 p.m. local time.

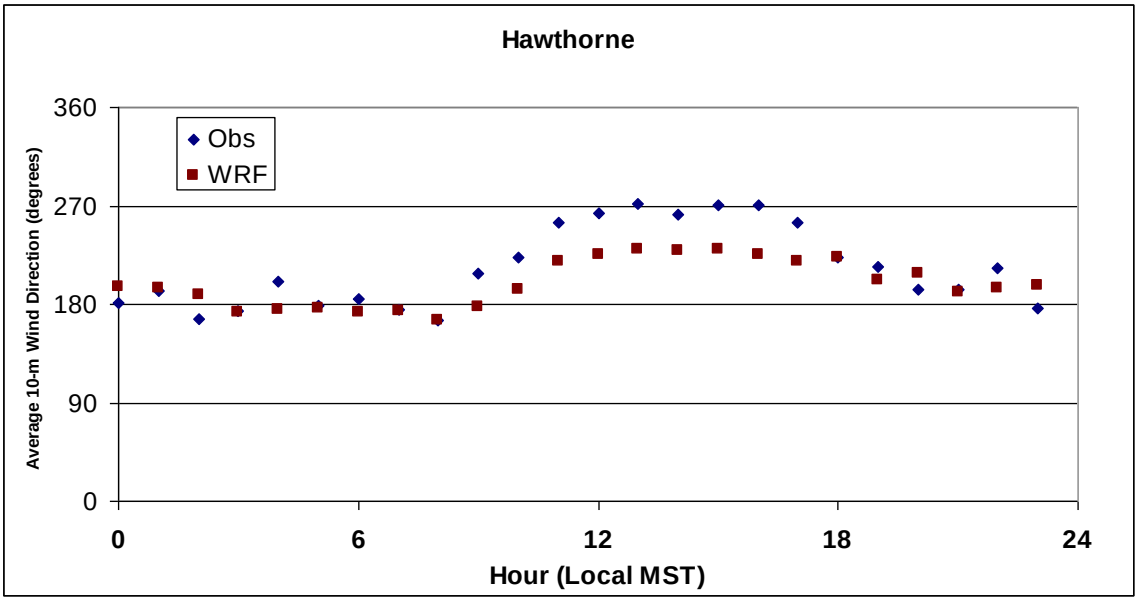

Figure 1.22: Averaged hourly WRF modeled 10-meter wind direction (red) and observed 10-meter wind direction (blue) at the Hawthorne monitor.

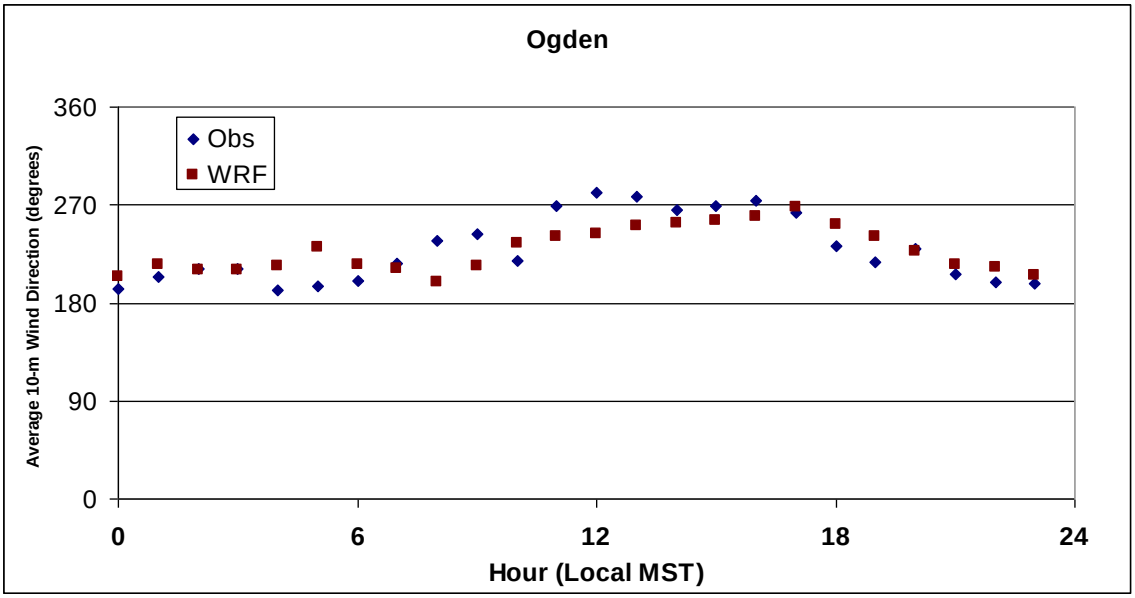

Figure 1.23: Averaged hourly WRF modeled 10-meter wind direction (red) and observed 10-meter wind direction (blue) at the Ogden monitor.

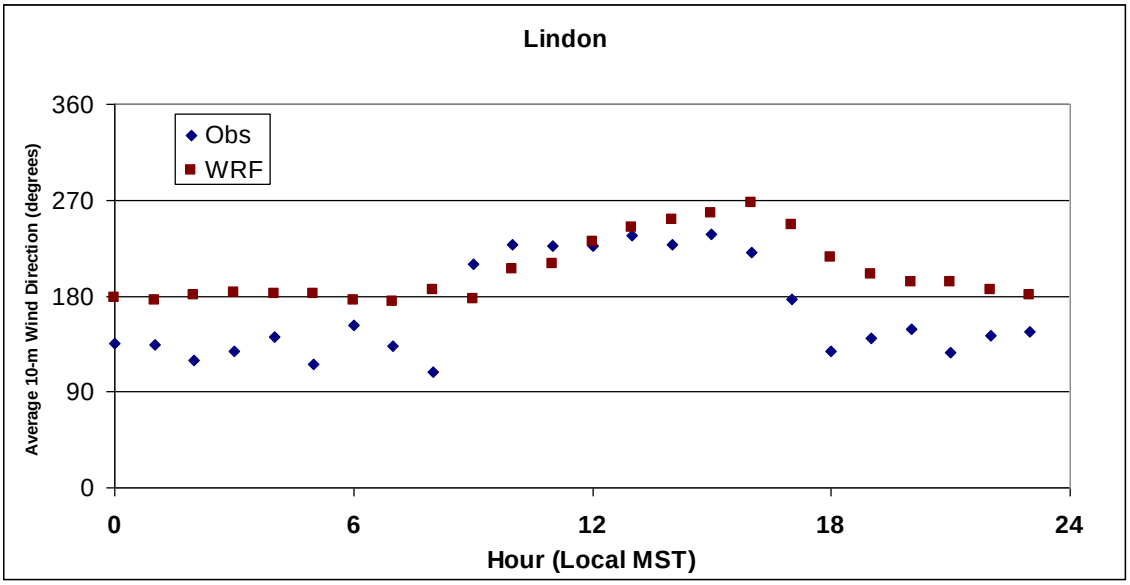

Figure 1.24: Averaged hourly WRF modeled 10-meter wind direction (red) and observed 10-meter wind direction (blue) at the Lindon monitor.

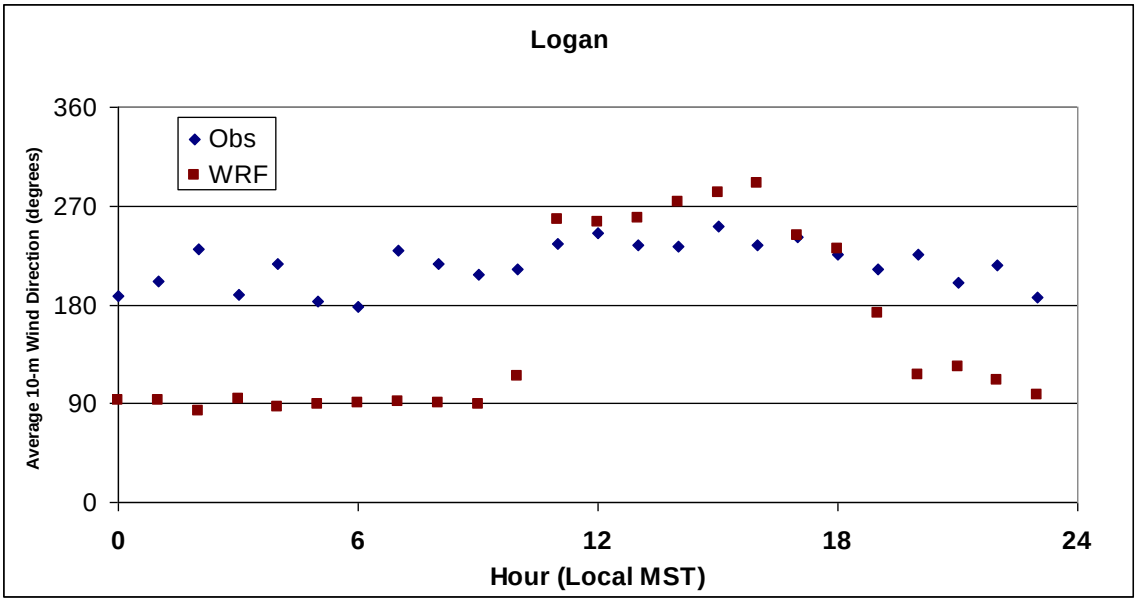

Figure 1.25: Averaged hourly WRF modeled 10-meter wind direction (red) and observed 10-meter wind direction (blue) at the Logan monitor.

An evaluation of statistic metrics for 10-m wind direction is presented in Table 1.7. For wind direction, bias and gross error are shown. The performance of WRF wind direction is good at Hawthorne and Ogden, with the gross error within the more restrictive Teshe, 2002 benchmark. Lindon performance is within the "complex terrain" benchmark. Logan misses the benchmarks, mainly due to the WRF nighttime downslope flow being easterly, instead of the observed southerly flow.

Table 1.8: WRF Performance for 10 meter wind direction.

	Statistic – Wind Direction (deg)	Benchmark (Teshe, 2002)	Complex Terrain Benchmark	WRF Values
Hawthorne	Bias	+- 10		-14
	Gross Error	<= 30	<= 55	**20**
Ogden	Bias	< +- 10		**-8**
	Gross Error	<= 30	<=55	**12**
Lindon	Bias	+- 10		38
	Gross Error	< =30	<= 55	**52**
Logan	Bias	+- 10		61
	Gross Error	<= 30	<= 55	77

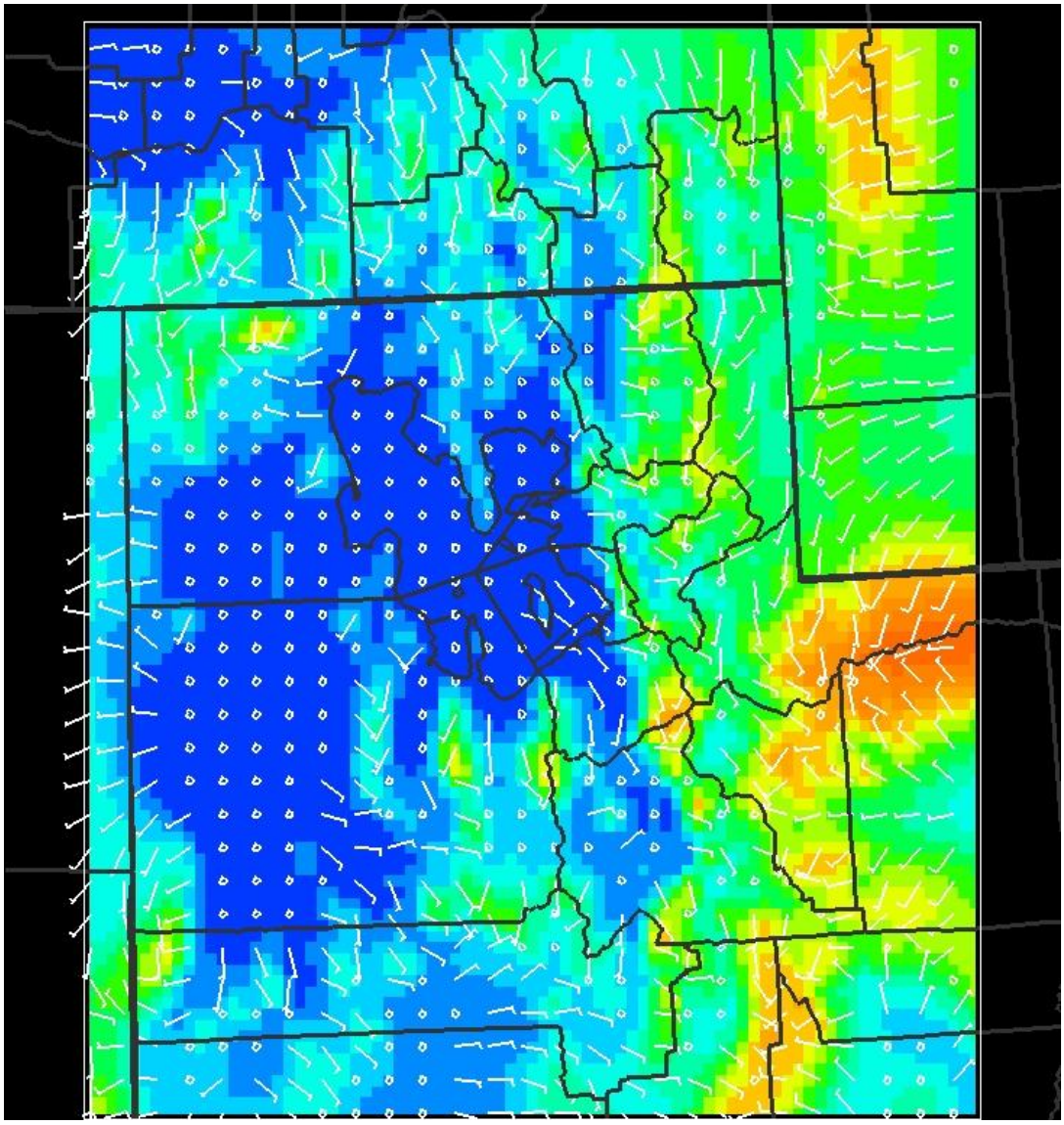

Figure 1.26: WRF wind direction (white wind barbs) and WRF topographic height (color-shaded) for 03 Jan. 2010 at midnight local time.

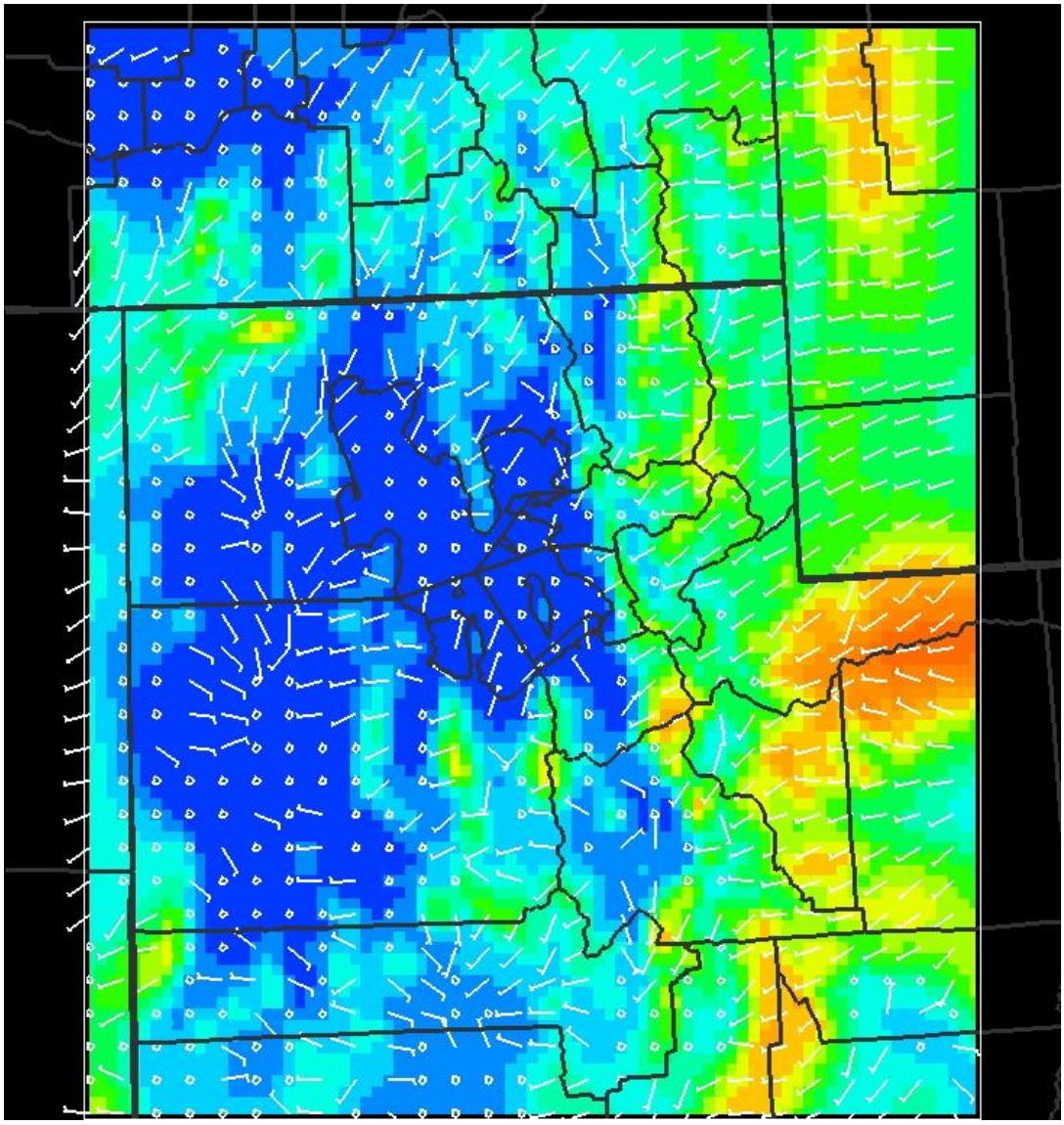

Figure 1.27: WRF wind direction (white wind barbs) and WRF topographic height (color-shaded) for 03 Jan. 2010 at 3 p.m. local time.

1.3 Weight of Evidence (WOE)/Supplementary Analysis

1.3.1 Ensemble WRF/MM5 Modeling

Prior to 2010, UDAQ worked with the Department of Army Dugway Proving Ground Meteorology Division for meteorological modeling services using NCAR's state of the Science MM5 & WRF modeling systems NCAR provided meteorological datasets from their Ensemble Real-Time Four Dimensional Data Assimilation (E-RTFDDA) model for a episode from 14-18 February 2008. This episode is not used in the Model Attainment demonstration. This modeling project was designed to investigate several difference WRF configurations with goal of finding an optimal setting to use for cold pool modeling.

The ensemble system consists of 30 members including 15 MM5 based members and 15 WRF based members. Table 1.9 gives an overview of all the model physics and initialization datasets the ensemble model allowed UDAQ to evaluate. Both analysis and observational nudging are used in all ensemble runs.

Table 1.9: The physical parameter suite used in NCAR's Ensemble Real-Time Four Dimensional Data Assimilation provided to UDAQ for February 2008 episode.

Physics	WRF	MM5
Cumulus	Kain-Fritsch Betts-Miller-Janic Grell-Devenyi	Kain-Fritsch Grell Betts-Miller-Janic Fritsch-Chappell Kuo
Microphysics	Kessler Lin et al. WSM5 WSM6 Thompson et al. Ferrier	Hsie Dudhia Ice Reisner 1 Reisner 2 Goddard Schwartz
Long-Wave Radiation	RRTM CAM GFDL	RRTM CCM2
Short-Wave Radiation	Dudhia Goddard CAM GFDL	Dudhia CCM2
PBL	YKU Meller-Yamada-Janic RUC GFS	MRF Blackadar Meller-Yamada-Janic Gyano-Seaman

Initialization Dataset	NAM GFS	NAM GFS
Other	No horizontal diffusion	No horizontal diffusion

Ensemble modeling performance for 2-m temperature is shown for Hawthorne (Figure 1.28) and Logan (Figure 1.29). The ensemble mean performs well at the Hawthorne monitor. This February episode was warmer than those often that occur in December and January and did not exhibit the decreasing surface temperature trend (Figure 1.9). This being a warmer episode may allow for better model performance for surface temperature. At Logan, almost all members of the ensemble miss the observed nighttime minimum temperatures (at hours ~ 48, 96, and 120 in the time series).

Ensemble modeling performance for 10-m wind speed is shown for Hawthorne (Figure 1.30) and Logan (Figure 1.31). After the initial frontal passage after the first 30 hours of the simulation, the ensemble mean wind speed performs quite well. Overall the ensemble mean nighttime wind speeds are biased high at night. Typically, the observed nighttime wind speed does not get over 3 mph throughout the episode while the majority of ensemble members have nighttime wind speeds between 3 and 5 mph. This nighttime wind bias is even greater at the Logan monitor (Fig. 1.31).

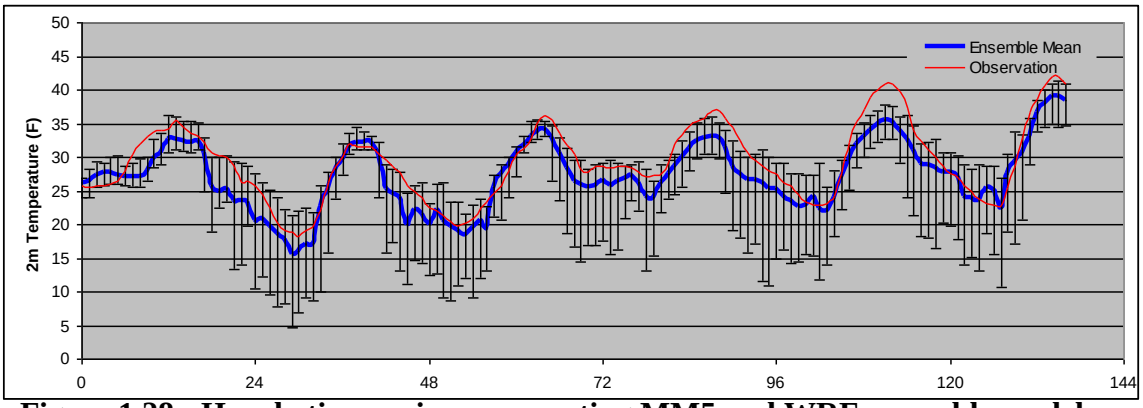

Figure 1.28: Hourly time series representing MM5 and WRF ensemble model performance for 2-m temperature for 14 – 19 Feb 2008 at the Hawthorne monitor. The 0 hour on the x-axis represents 14 Feb 2008 at 00 Local Mountain Time. The model ensemble Mean (blue) and observations (red) are shown. The black bars give the spread of ensemble members.

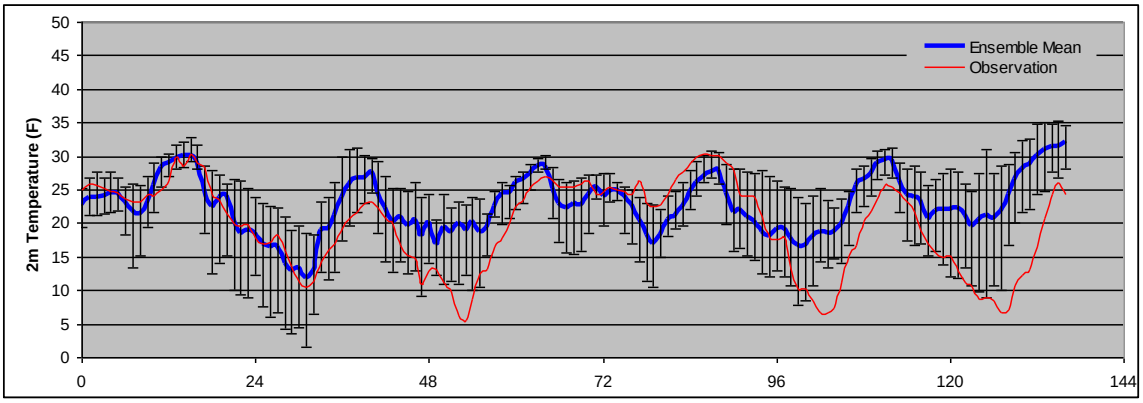

Figure 1.29: Hourly time series representing MM5 and WRF ensemble model performance for 2-m temperature for 14 – 19 Feb 2008 at the Logan monitor. The 0 hour on the x-axis represents 14 Feb 2008 at 00 Local Mountain Time. The model ensemble Mean (blue) and observations (red) are shown. The black bars give the spread of ensemble members.

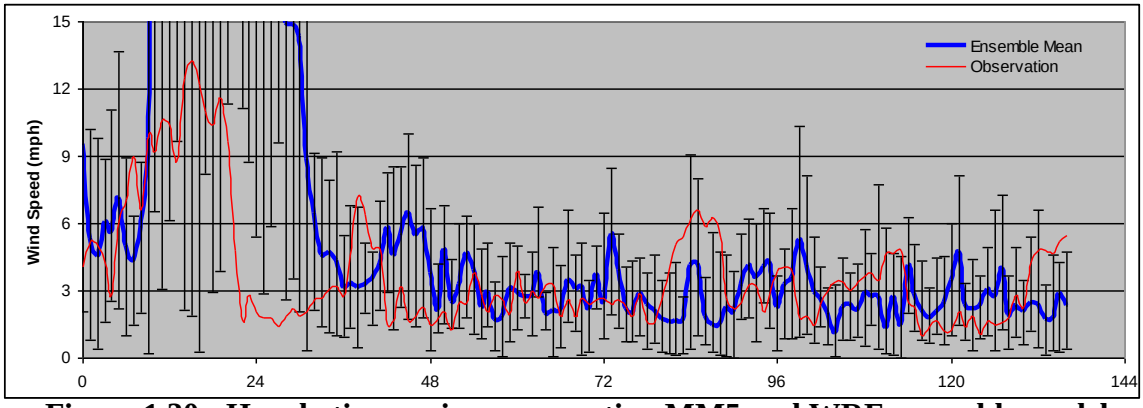

Figure 1.30: Hourly time series representing MM5 and WRF ensemble model performance for 10-m wind speed for 14 – 19 Feb 2008 at the Hawthorne monitor. The 0 hour on the x-axis represents 14 Feb 2008 at 00 Local Mountain Time. The model ensemble Mean (blue) and observations (red) are shown. The black bars give the spread of ensemble members.

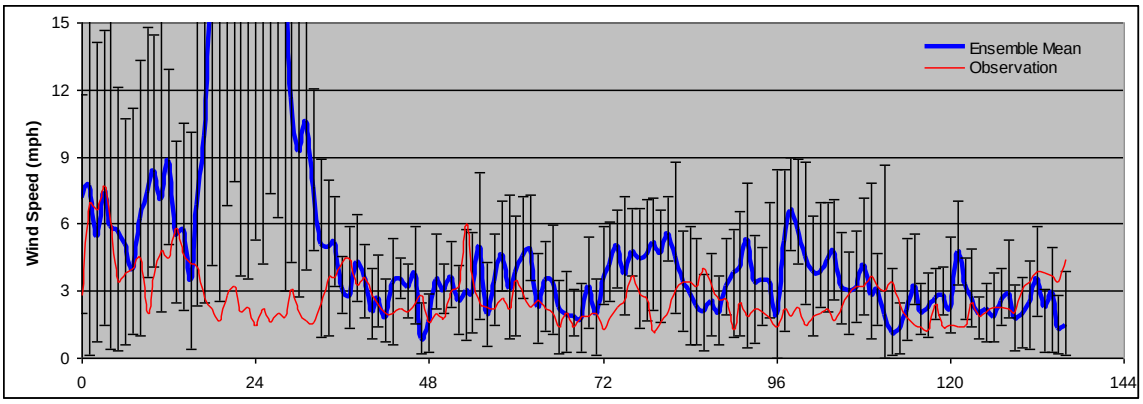

Figure 1.31: Hourly time series representing MM5 and WRF ensemble model performance for 10-m wind speed for 14 – 19 Feb 2008 at the Logan monitor. The 0 hour on the x-axis represents 14 Feb 2008 at 00 Local Mountain Time. The model ensemble Mean (blue) and observations (red) are shown. The black bars give the spread of ensemble members.

1.3.2 Meteorological Modeling Sensitivities

In addition to the ensemble provided by NCAR, UDAQ performed numerous sensitivities to test WRF's ability to better simulate Utah's wintertime conditions. One sensitivity that UDAQ spent a considerable amount of resources on was to test the horizontal and vertical resolution in WRF. UDAQ modeled the Cache Valley (Logan NAA) at horizontal resolution at 1.33 km for the innermost domain. No improvement was seen in WRF's capability to model cold pool situations, especially in its performance of surface temperature.

Numerous attempts were made to assess the effect of increasing vertical resolution. UDAQ replicated modeling work performed for the Fairbanks, AK NAA. This work included WRF being run with very high vertical resolution near the surface - five vertical layers within the first 20 meters. This simulation, as well as others performed by UDAQ, showed limited benefit from increasing the vertical resolution.

Additional WRF sensitivities performed by UDAQ:

- Tested influence of Pleim-Xiu, RUC, and Noah Land Surface Models.
- Tested eddy diffusion in the PBL by examining minimum eddy diffusivity (Kv) and friction velocity.
- Limited horizontal diffusion.
- Tested influence of initialization dataset (NAM, GFS)

The additional WRF sensitivities provided different performance for surface temperatures, winds, and vertical structure. However, none led to a noticeably better performance of the surface temperature during cold pools (as described in Section 1.2.3).

1.4 Summary

Model performance of WRF was assessed against observations at sites maintained by the Utah Air Monitoring Center. A summary of the performance evaluation results for WRF are presented below:

- The biggest issue with meteorological performance is the existence of a warm bias in surface temperatures during high PM2.5 episodes. This warm bias is common trait of WRF modeling of during Utah wintertime inversions.

- WRF does a good job replicating the light wind speeds (< 5 mph) that occur during high PM2.5 episodes.

- WRF is able simulate the diurnal wind flows common during high PM2.5 episodes. WRF captures the overnight downslope and daytime upslope wind flow that occurs in Utah valley basins.

- WRF has reasonable ability to replicate the vertical temperature structure of the boundary layer (i.e., the temperature inversion). Although it is difficult for WRF to reproduce the extreme stability of the inversion when it is shallow and strong (i.e., an 8 degree temperature increase over 100 vertical meters). Also, WRF mixes out the boundary layer temperature stability at the end of high PM2.5 episodes, leading to poor model performance. These modeling days that exhibit poor performance are excluded from the model attainment test.